C-terminal proteolysis of the collagen VI α3 chain by BMP-1 and proprotein convertase(s) releases endotrophin in fragments of different sizes

Stefanie Elisabeth Heumüller, Maya Talantikite, Manon Napoli, J. Armengaud, Matthias Mörgelin, Ursula Hartmann, Gerhard Sengle, Mats Paulsson, Catherine Moali, Raimund Wagener

C-terminal proteolysis of the collagen VI α3 chain by BMP-1 and proprotein convertase(s) releases endotrophin in fragments of different sizes

Received for publication, March 28, 2019, and in revised form, July 23, 2019 Published, Papers in Press, July 25, 2019, DOI 10.1074/jbc.RA119.008641

Stefanie Elisabeth Heumüller[‡1], Maya Talantikite[§1], Manon Napoli[§], Jean Armengaud[¶], Matthias Mörgelin[‖], Ursula Hartmann[‡], Gerhard Sengle[‡‡‡§§], Mats Paulsson[‡**‡‡¶¶], Catherine Moali[§2,3], and Raimund Wagener[‡**‡‡2,4]**

*From the [‡]Center for Biochemistry, Faculty of Medicine, the [‡‡]Center for Molecular Medicine Cologne (CMMC), and the [¶¶]Cluster of Excellence Cellular Stress Responses in Aging-Associated Diseases (CECAD), University of Cologne, 50931 Cologne, Germany, the [§]Tissue Biology and Therapeutic Engineering Laboratory, UMR5305 CNRS/University of Lyon, 69367 Lyon, France, the [¶]Commissariat à l'Energie Atomique (CEA)-Marcoule, DRF/JOLIOT/DMTS/SPI/Li2D, Innovative Technologies for Detection and Diagnostics Laboratory, 30200 Bagnols-sur-Cèze, France, [‖]Colzyx AB, Medicon Village, SE-223 81 Lund, Sweden, the **Cologne Center for Musculoskeletal Biomechanics (CCMB), 50931 Cologne, Germany, and the [§§]Department of Pediatrics and Adolescent Medicine, Experimental Neonatology, Faculty of Medicine and University Hospital Cologne, 50931 Cologne, Germany*

Edited by Paul E. Fraser

The assembly of collagen VI microfibrils is a multistep process in which proteolytic processing within the C-terminal globular region of the collagen VI α3 chain plays a major role. However, the mechanisms involved remain elusive. Moreover, C5, the short and most C-terminal domain of the α3 chain, recently has been proposed to be released as an adipokine that enhances tumor progression, fibrosis, inflammation, and insulin resistance and has been named "endotrophin." Serum endotrophin could be a useful biomarker to monitor the progression of such disorders as chronic obstructive pulmonary disease, systemic sclerosis, and kidney diseases. Here, using biochemical and isotopic MS-based analyses, we found that the extracellular metalloproteinase bone morphogenetic protein 1 (BMP-1) is involved in endotrophin release and determined the exact BMP-1 cleavage site. Moreover, we provide evidence that several endotrophin-containing fragments are present in various tissues and body fluids. Among these, a large C2–C5 fragment, which contained endotrophin, was released by furin-like proprotein convertase cleavage. By using immunofluorescence microscopy and EM, we also demonstrate that these proteolytic maturations occur after secretion of collagen VI tetramers and during microfibril assembly. Differential localization of N- and C-terminal regions of the collagen VI α3 chain revealed that cleavage products are deposited in tissue and cell cultures. The detailed information on the processing of the collagen VI α3 chain reported here provides a basis for unraveling the function of endotrophin (C5) and larger endotrophin-containing fragments and for refining their use as biomarkers of disease progression.

Collagen VI is a microfibrillar collagen present in the extracellular matrix of most tissues. It is thought to support tissue architecture and to anchor large interstitial structures. Collagen VI is unusual in the collagen family in having only a short triple helical region with most of the molecule being made up by von Willebrand factor A (VWA)[5] domains that may be involved in many intra- and intermolecular interactions (1). There are altogether six collagen VI α-chains, designated α1–α6. Among these, the α1–α3 chains were first identified and occur in most collagen VI molecules. Based on sequence similarity, the α4–α6 chains were later detected (2, 3) and found to be constituents of alternatively assembled collagen VI molecules, where they replace the α3 chain (4). Their tissue distributions are more restricted than those of the α1–α3 chains (5). In humans, the α4 chain is absent, due to a large pericentric inversion on chromosome 3 interrupting the *COL6A4* gene (6).

Much information on collagen VI function has been gained by studying a mouse model in which the *Col6a1* gene is inactivated (7). As the α1 chain is an obligatory constituent of all collagen VI molecules, its loss leads to a complete lack of assembled molecules. These mice are fertile and surprisingly normal in general appearance. Still, upon closer examination, they display a number of important functional phenotypes. Most prominently, they show an early onset myopathy, with similarities to human Bethlem myopathy (7). In the myofibers, mito-

This study was supported by German Research Council Grants SFB 829-B2 and FOR 2722-B1 (to R. W. and M. P.) and Grants SFB829/B11 and B12 and FOR 2722-M2 (to G. S.), by the Région Rhône-Alpes Auvergne (to M. T. and C. M.), and by CNRS and the University of Lyon (to C. M.). The authors declare that they have no conflicts of interest with the contents of this article.

This article contains Figs. S1 and S2.

[1] Both authors contributed equally to this work.

[2] Both authors contributed equally to this work.

[3] To whom correspondence may be addressed: Tissue Biology and Therapeutic Engineering Laboratory (LBTI), 7, Passage du Vercors, 69367 Lyon Cedex 7, France. Tel.: 33-472-722-638; Fax: 33-472-722-604; E-mail: catherine.moali@ibcp.fr.

[4] To whom correspondence may be addressed: Institute for Biochemistry II, Faculty of Medicine, University of Cologne, Joseph-Stelzmann-Str. 52, D-50931 Cologne, Germany. Tel.: 49-221-478-6990; Fax: 49-221-478-6977; E-mail: raimund.wagener@uni-koeln.de.

[5] The abbreviations used are: VWA, von Willebrand factor A; AEBSF, 4-(2-aminoethyl)benzenesulfonyl fluoride hydrochloride; TAILS, terminal amine isotopic labeling of substrates; ATOMS, amino-terminal oriented mass spectrometry of substrates; PC, proprotein convertase; BMP, bone morphogenetic protein; COPD, chronic obstructive pulmonary disease; TBS, Tris-buffered saline; BisTris, 2-[bis(2-hydroxyethyl)amino]-2-(hydroxymethyl)propane-1,3-diol; DMEM, Dulbecco's modified Eagle's medium; AGC, automatic gain control; EM, electron microscopy.

chondrial dysfunction (8) and organelle alterations are caused by defects in the autophagic pathway (9). Further, the neuromuscular junction is affected, leading to electrophysiological defects (10). In cell cultures of central neurons derived from *Col6a1*$^{-/-}$ mice, increased apoptosis was observed, indicating a neuroprotective effect of the protein (11). In the peripheral nervous system, hypermyelination (12) and impaired injury-induced nerve regeneration (13) were detected. The mice also have skeletal phenotypes with accelerated development of osteoarthritis, delayed secondary ossification, reduced bone mineral density (14, 15), and distorted osteoblast shape (16). In skin, there are no overt defects, but a decrease in tensile strength (17) and changes in hair growth (18). Further phenotypes have been described in heart (19), tendon (20), and lung (21). It is uncertain whether these changes are caused by loss of the structural role of collagen VI, loss of its signaling functions, or both.

The α3 chain of collagen VI is known to undergo proteolysis in a time- and tissue-specific manner (22–25). Also, proteolytic fragments from the C-terminal part of this chain have been proposed to have signaling effects, including pro-fibrotic features and macrophage chemoattractant properties (22, 26). They also promote cancer progression and cause chemoresistance of cancer cells (27). This part of the α3 chain consists of two VWA domains (C1 and C2), a unique domain (C3), a fibronectin type III repeat (C4), and, at the very C terminus, a Kunitz domain (C5). This C5 domain was suggested to be a major mediator of collagen VI signaling and was named endotrophin (22). The C5 domain is needed for collagen VI microfibril formation (28), from which it is later cleaved off (23, 24), and it was shown that C5 is a ligand for the anthrax receptor 1 (also known as tumor endothelial marker 8, or TEM8) (29). However, the nature of the released fragments containing the C5 domain is not known, and the cleavage sites used and the proteases responsible have not been identified. We therefore performed the present study to resolve the *in vivo* biogenesis and precise tissue localization of endotrophin.

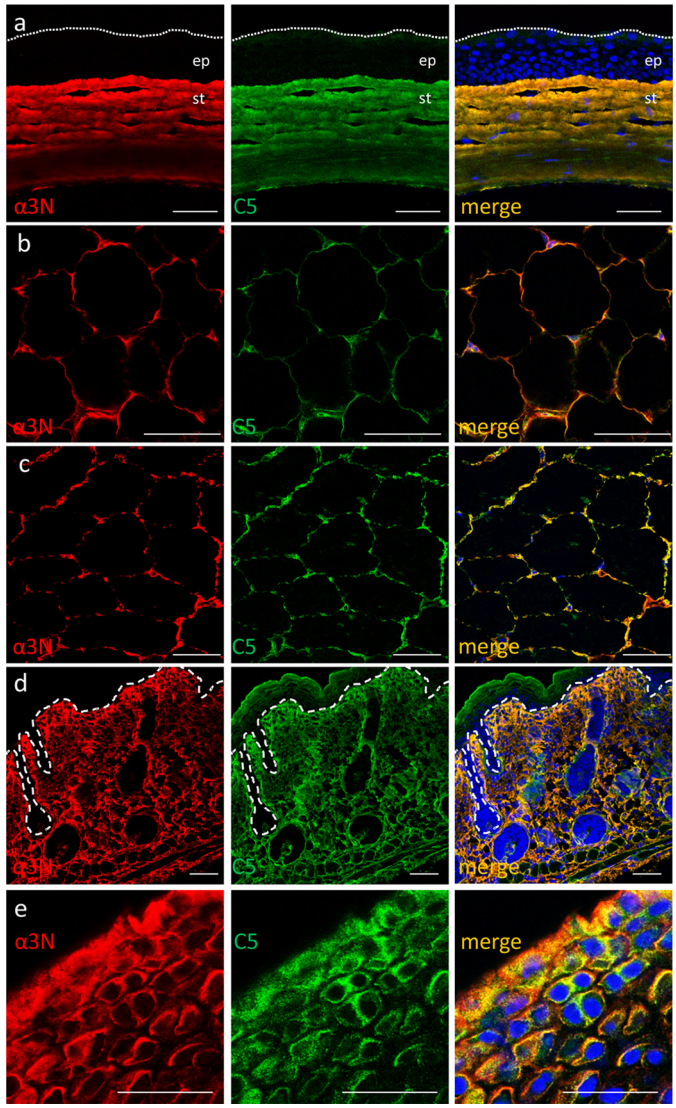

Figure 1. Overlapping and differential tissue localization of the N- and C-terminal epitopes of the collagen VI α3 chain. Immunofluorescence microscopy was performed on frozen (*a*, *c*, *d*, and *e*) or paraffin-embedded sections (*b*) from murine cornea (*a*), white adipose tissue (*b*), muscle (*c*), skin (*d*), and knee articular cartilage (*e*). Shown are adult (*a* and *b*) and newborn mice (*c*–*e*). Sections were incubated with the affinity-purified antibodies against the collagen VI α3 N terminus (*red*) and C5 (*green*); merge is shown in *yellow*. *ep*, epithelium, *st*, stroma. In *a*, the upper margin of the epithelium is indicated by a *dotted line*, and in *d*, the dermal/epidermal basement membrane is shown by a *dashed line*. *Bars*, 25 μm in *e* and 50 μm in *a*–*d*.

Results

Differential localization of N- and C-terminal parts of the collagen VI α3 chain

Proteolytic processing of the noncollagenous C-terminal part of the collagen VI α3 chain has been reported (22–25), but the tissue localizations of the unprocessed α3 chain and its cleavage products, especially the C5 domain (endotrophin), have not been extensively studied. Therefore, immunostainings using affinity-purified antibodies against the N2–N9 domains and the C5 domain of the α3 chain were performed. The antibody against the N terminus detects all α3 chains, whereas the C5 antibody reveals the full-length α3 chain and cleavage products that contain the C5 domain (Fig. S1). Interestingly, the staining patterns obtained with the two antibodies and their degrees of overlap vary between tissues. Whereas in the cornea, the staining with the antibodies against the N- and C termini mostly overlaps (Fig. 1*a*), in white adipose tissue (Fig. 1*b*), skeletal muscle (Fig. 1*c*), skin (Fig. 1*d*), and knee articular cartilage (Fig. 1*e*), a partially differential localization is observed. In white adipose and skeletal muscle tissue, the staining is often overlapping, but also areas are stained preferentially by either N- or C-terminal antibodies. In skin, both antibodies label a dense fibrous network throughout the dermis, whereas structures around hair follicles and just below the dermal epidermal basement membrane and the matrix surrounding subcutaneous fat cells are almost exclusively stained with the C-terminal antibody. Moreover, in articular cartilage, a strong pericellular labeling around chondrocytes is observed with both N- and C-terminal antibodies. However, in the direct vicinity of the chondrocytes, a stronger staining by the C-terminal antibody is often observed. The differential staining indicates that, in certain locations, C-terminal cleavage products of the α3 chain

occur with a higher abundance than the N-terminal part of the processed α3 chain.

C-terminal cleavage products of the collagen VI α3 chain vary in size, and their composition is tissue-specific

The differential staining pattern obtained by antibodies directed against either N- or C-terminal parts of the collagen VI α3 chain prompted us to characterize the proteolytic processing at the C terminus in different tissues and body fluids by immunoblotting using the affinity-purified antibody against C5, the most C-terminal domain (Fig. 2, *a* and *b*). Interestingly, a fragment corresponding to the ~8-kDa free C5 domain (endotrophin) proved difficult to detect. Only after overexposure, very weak signals were detected in extracts of white adipose tissue, skeletal muscle, and skin (Fig. 2*b*). A somewhat stronger signal of corresponding size was detected in amniotic fluid, but not in serum or urine. However, a variety of larger C5-containing fragments, ranging in size from about 25 to 120 kDa, were found in body fluids and tissue extracts (Fig. 2*a*) with a great diversity in fragment size and abundance between sources. Strong signals and a complex band pattern were seen in skeletal muscle, white adipose tissue, cartilage, and amniotic fluid, whereas skin, cornea, and serum showed weaker signals and less complex band patterns, and in urine, no signals could be obtained. Interestingly, in serum, only a single fragment was detected, which has the same mobility as the recombinant C2–C5 (~100 kDa; Fig. 2*d*) and is apparently also found in muscle, cartilage, amniotic fluid, and white adipose tissue. The results clearly show that free endotrophin (C5) is a very minor component among the C-terminal cleavage products of the α3 chain. Moreover, as the antibody is directed against C5 at the very C-terminal end of the α3 chain, the sizes of the fragments obtained could be used to derive sequence regions in which cleavage probably occurs (Fig. 2, *c* and *d*) (*e.g.* the prominent band that runs at around 25 kDa most likely consists of the fibronectin type III repeat and the C5 Kunitz domain, and the cleavage site must be located at the C terminus of the unique domain).

Identification of proteinases involved in the release of C5/endotrophin-containing fragments

In the course of a parallel study aiming at identifying novel substrates of the BMP-1 (bone morphogenetic protein 1) metalloproteinase, we found that the collagen VI α3 chain was a candidate substrate. Using the TAILS (terminal amine isotopic labeling of substrates (30)) proteomic approach to analyze the conditioned medium of primary human corneal keratocytes, we could identify the TEPLALTETDICK peptide as a BMP-1–derived neo-N terminus that was unambiguously assigned to the C terminus of the α3 chain (Table 1). In two different experimental settings (in culture and after *in vitro* incubation of keratocyte supernatant with exogenous recombinant BMP-1), this peptide was detected by tandem MS as more abundant in the presence of the protease (endogenous or recombinant BMP-1) than in inhibitor-treated samples, thereby defining a putative BMP-1 cleavage site between Ser^{3100} and Thr^{3101} of the human α3 chain (numbering according to the α3 chain NCBI Reference Sequence NP_004360.2). This cleavage site is located

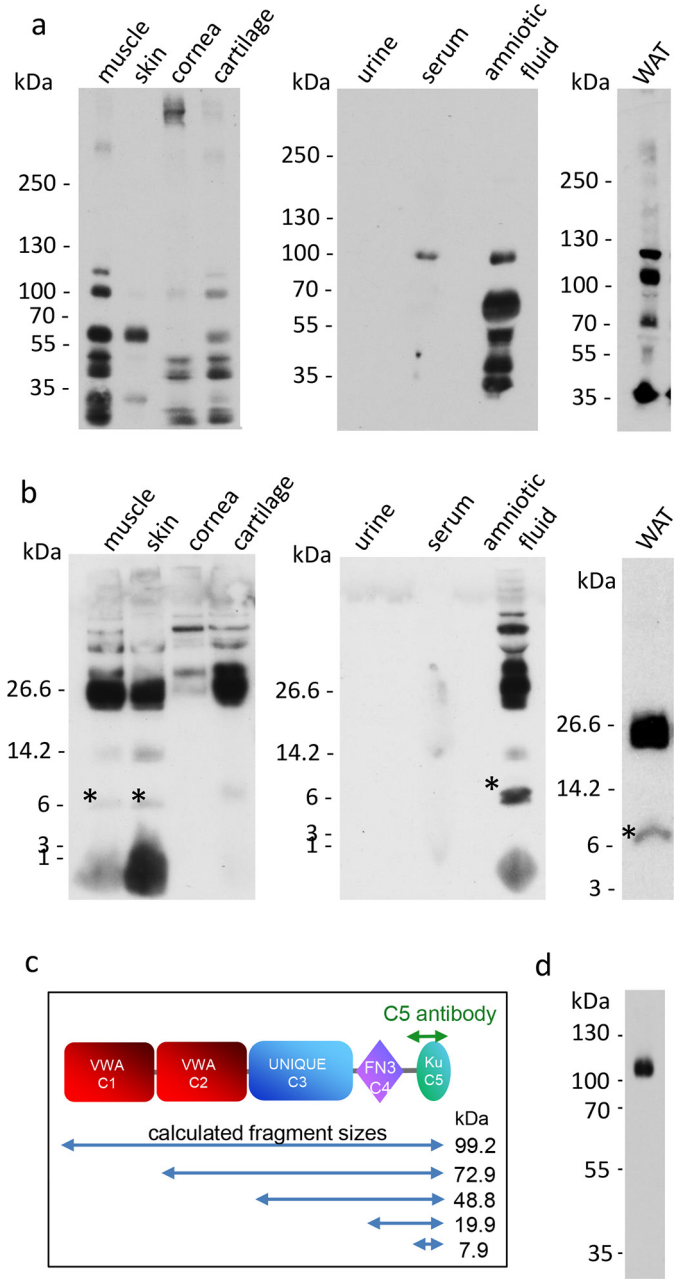

Figure 2. C5-containing fragments of the collagen VI α3 chain are of diverse sizes. Tissue extracts and body fluids were subjected to SDS-PAGE on Tris-glycine 4–12% polyacrylamide gradient gels (*a*) and on 12% BisTris polyacrylamide gels (*b*) under nonreducing conditions. Proteins were transferred to a membrane and detected with affinity-purified antibodies against the C5 domain. *, bands that run at the position expected for cleaved off endotrophin. *c*, domain structure of the C terminus of the collagen VI α3 chain with calculated fragment sizes indicated. *FN3*, fibronectin-type III repeat; *Ku*, Kunitz domain. *d*, mobility of recombinant mouse collagen VI α3 chain C2–C5 fragment (Ala^{2608}–Val^{3284}) on a Tris-glycine 8% polyacrylamide gel. *WAT*, white adipose tissue.

some residues before the predicted border of the C5 domain and could define the N terminus of the small fragment (~8 kDa) (endotrophin) detected in tissues and cell culture supernatants (Figs. 2*b* and 3*a*).

The possibility that BMP-1 cleaves the collagen VI α3 chain was confirmed by immunoblotting using the antibody directed against the C5 domain. A larger amount of a product migrating below 10 kDa upon SDS-PAGE was detected when keratocyte

Table 1

High-confidence peptide with N-terminal iTRAQ from the C1–C5 domains of the human collagen VI α3 chain (Uniprot accession number P12111) identified by TAILS in the conditioned medium of human primary keratocytes

Two ratios were calculated from a 4-plex experiment and correspond to the comparison of (i) two conditions where cells were grown in the presence of a BMP-1 inhibitor or DMSO vehicle (DMSO/inhibitor) and (ii) two conditions where the conditioned medium of keratocytes was incubated with recombinant BMP-1 or BMP-1 inhibitor (BMP-1/inhibitor).

Peptide	Position (number of peptide identifications)	iTRAQ ratios	
		DMSO/inhibitor (in culture)	BMP-1/inhibitor (*in vitro*)
TEPLALTETDICK	3101–3113 (2)	2.38 ± 0.01	6.32 ± 0.26

supernatant was incubated in the presence of recombinant BMP-1 (under the same conditions as the TAILS *in vitro* assay; Fig. 3*a*). Further confirmation of the cleavage was obtained by *in vitro* cleavage assays using purified recombinant BMP-1 and a recombinant α3 chain C-terminal fragment harboring an extended C5 domain including a sequence of 32 amino acid residues containing the BMP-1 cleavage site identified by TAILS (recombinant hC5). This protein was completely cleaved after 4 h in the presence of BMP-1, at two different molar ratios, which generated a fragment similar in size to the previously described 8-kDa product (Fig. 3*b*; a second proteolysis product was too small to be resolved). A corresponding mouse protein (recombinant mC5) was also cleaved with BMP-1, and the products were subjected to MS analysis using the ATOMS (amino-terminal oriented mass spectrometry of substrates) technique (31, 32). This revealed that the cleavage occurs at a position corresponding to that in the human protein (Fig. 3*c*), between Asn^{3216} and Thr^{3217} (based on the α3 chain NCBI Reference Sequence NP_001229937.1), despite the incomplete conservation of the cleavage site (Asn instead of Ser in the P1 position). It is noteworthy that both the human and mouse cleavage sites differ from the known consensus sequence for BMP-1 cleavage. BMP-1 is usually described to have a strong preference for aspartate in the P1′ position, but this is not exclusive, and several reports have now shown that BMP-1 can also efficiently cleave substrates with glutamate (31), glutamine (33, 34), and threonine (35) in this position. Importantly, IGFBP3 was previously shown to be cleaved by BMP-1 between a serine and a threonine (35), exactly like the human collagen VI α3 chain, unequivocally establishing threonine as a preferred residue in the P1′ position for the BMP-1 protease.

Thorough analysis of mouse and human α3 chain sequences revealed that both also contain a putative cleavage site for proprotein convertases (PC; *e.g.* furin) located between the C1 and the C2 domain. In agreement with this observation, a recombinant mouse C1–C5 construct produced in HEK 293-EBNA cells with a C-terminal One-STrEP tag reproducibly co-purified in affinity chromatography with a cleavage product that has the same mobility as recombinant C2–C5 (Fig. 2*d*) by SDS-PAGE. This co-purified fragment was then shown by MS to start with Ala-2608, which is located just after the RDRR (amino acids 2604–2607) sequence defining a canonical PC cleavage site. Finally, we found that this cleavage site is also utilized in cell cultures of mouse primary dermal fibroblasts, leading to the generation of a similar fragment of around 100 kDa, which was completely prevented in the presence of a furin inhibitor (Fig. 3*d*).

In summary, we have identified two proteinases that cleave the α3 chain between the C1 and C2 domains (furin-like proprotein convertase) and between the C4 and C5 domains (BMP-1). The action of these generates at least part of the complex fragment patterns found in tissues.

Collagen VI tetramers are secreted as full-length proteins and processed after microfibril assembly

The C5 domain of the collagen VI α3 chain is critical for extracellular microfibril formation and is present in the extracellular matrix of SaOS-2 cells and fibroblasts (28). In cartilage, the C5 domain is cleaved off from collagen VI microfibrils immediately after secretion (23). However, the time course of the processing and microfibril assembly is unclear. Therefore, we studied the different steps of assembly and cleavage in cultures of primary dermal fibroblasts between days 1 and 6 of culture (Figs. 4 and 5 and Fig. S2). Already at day 1, a matrix is laid down on the cell culture dish that becomes more dense in the following days. At all times (representative images are shown for day 4 in Fig. 4*a*), three different networks can be distinguished. The first is stained only by the antibody detecting the N terminus of the collagen VI α3 chain representing a mature collagen VI microfibrillar network. A second network is stained by antibodies both against the N terminus and the C5 domain of the α3 chain (Fig. 4*a*), indicating that a proportion of the C5 domains are still attached to the α3 chains in the microfibrillar network, indicating immature assemblies of collagen VI microfibrils. The presence of both of these networks at all time points indicates that the maturation of collagen VI microfibrils is a continuous process that starts immediately when collagen VI is secreted. Interestingly, a third network exists that is stained only by the antibody against the C5 domain, indicating the matrix deposition of C5-containing fragments independent of collagen VI microfibrils.

To clearly show that also collagen VI tetramers still contain the C5 domain when secreted, we performed composite SDS-polyacrylamide-agarose gel electrophoresis and indeed identified C5-containing tetramers by immunoblotting (Fig. 4*b*). We further studied the cleavage of the C terminus from collagen VI microfibrils in the supernatant of cultured primary fibroblasts by immunoelectron microscopy using antibodies against the α3 chain N terminus or the C5 domain labeled with gold particles of different sizes (Fig. 5*a*). The supernatant contains a fraction of semisoluble particles encompassing small immature and mature microfibrils and cleavage products thereof. In early cultures (24 h), collagen VI microfibrils carried gold particles located at the globular parts (Fig. 5*a*). However, whereas the labeling with the antibody against the N terminus remained also at later stages of culture (6 days), labeling with the C5 antibody gradually disappeared, indicating an increasing concentration of mature microfibrils in the supernatant. Most of the gold-labeled C5 antibodies were located either close to the triple-helical part or at some distance from the microfibrils (Fig. 5, *a* and *b*). Between day 1 and day 6, the proportion of C5 antibodies located on microfibrils decreased, and the cleaved off

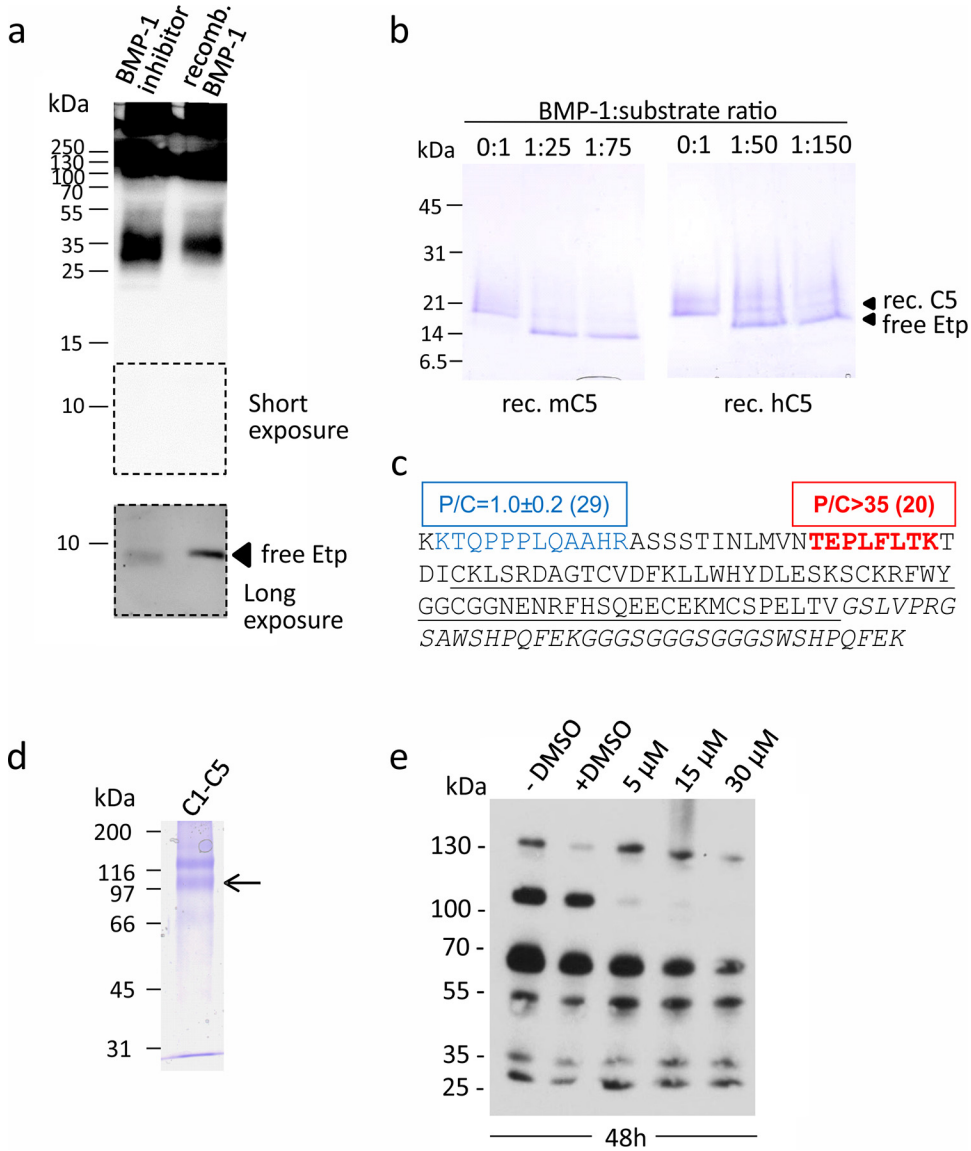

Figure 3. BMP-1 and furin-like proprotein convertase(s) contribute to the processing of the C-terminal part of the collagen VI α3 chain. *a*, immunoblot of keratocyte conditioned medium incubated with 10 μM BMP-1 inhibitor or 0.27 μg of recombinant BMP-1 (protease/total protein ratio 1:100) for 2 h at 37 °C. Proteins were submitted to SDS-PAGE on a 15% Tris-glycine polyacrylamide gel under nonreducing conditions and detected with an antibody against human endotrophin (C5; *Etp*). *b*, cleavage assays with purified recombinant human and mouse collagen VI α3 chain C5 proteins (carrying an N-terminal extension harboring the BMP-1 cleavage site) and BMP-1. Incubation was at 37 °C for 4 h, and detection was by SDS-PAGE on a 4–20% Tris-glycine polyacrylamide gradient gel (reducing conditions) and Coomassie Blue staining. *c*, summary of the results from the ATOMS experiment performed with the mouse collagen VI α3 C5 protein (rec. mC5). Positions of identified peptides in the protein sequence are shown (*P/C*, protease/control ratio (mean ± S.D.); the *number* in *brackets* indicates the number of peptides used for quantification; *underlined* is the sequence of the C5 domain as defined in Uniprot; Strep-tag sequence in *italics*). *d*, Coomassie Blue–stained SDS-PAGE (8% Tris-glycine polyacrylamide gradient gels under nonreducing conditions) of affinity-purified C-terminally Strep-tagged C1–C5. The *arrow* indicates the proprotein convertase cleaved band. *e*, immunoblot of supernatants from primary dermal fibroblasts cultured in the absence or presence of 5, 15, or 30 μM furin inhibitor I for 48 h. The samples were analyzed on a 4–12% Tris-glycine polyacrylamide gradient gel under nonreducing conditions, transferred to a membrane, and detected with the affinity-purified antibody against the mouse collagen VI α3 chain C5 domain.

fragments accumulated on the grids on areas between microfibrils. This shows that processing occurs after secretion of tetramers and that release of C5 from freshly assembled microfibrils, at least under cell culture conditions, is a continuous process.

Discussion

Research on collagen VI has long been focused on the complex assembly and function of the microfibrils and on the pathomechanism of collagen VI–related myopathies. Proteolytic processing at the C terminus of the α3 chain was not studied in greater detail, and the exact cleavage sites were hitherto not known. However, it was shown that C5, the most C-terminal domain, is necessary for fibril formation (28) and that mature microfibrils lack C2–C5 (24), which indicates that processing is part of the maturation of microfibrils. In addition, a novel cytokine-like function for the cleaved-off 8-kDa C5 domain, endotrophin, was proposed. Endotrophin is assumed to be released in white adipose tissue and to act as an adipokine (22). In mice, it enhances breast tumor progression, increases fibrosis and inflammation, and ultimately leads to enhanced insulin resistance (26). However, there is no published evidence

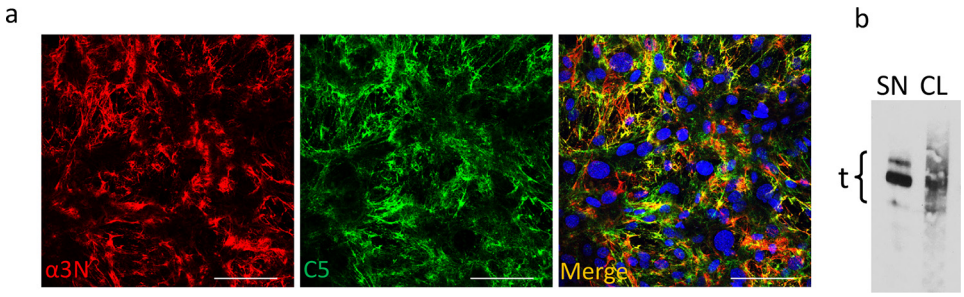

Figure 4. Fibroblasts secrete collagen VI tetramers containing the C5 domain of the collagen VI α3 chain. Primary dermal fibroblasts isolated from newborn mice were cultured for 4 days. *a*, immunofluorescence microscopy with antibodies against the N terminus (*red*) and the C5 domain (*green*) of the collagen VI α3 chain. *Bar*, 100 μm. *b*, immunoblot of the collagen VI tetramers in cell lysate (*CL*) and supernatant (*SN*) separated under nonreducing conditions on a composite agarose-polyacrylamide (0.5%/2.4%) gel. Purified murine collagen VI tetramers were used as a marker (not shown). The loading buffer contained 2 M urea. Collagen VI tetramers were detected with an affinity-purified antibody against the collagen VI α3 chain C5 domain. *t*, tetramers.

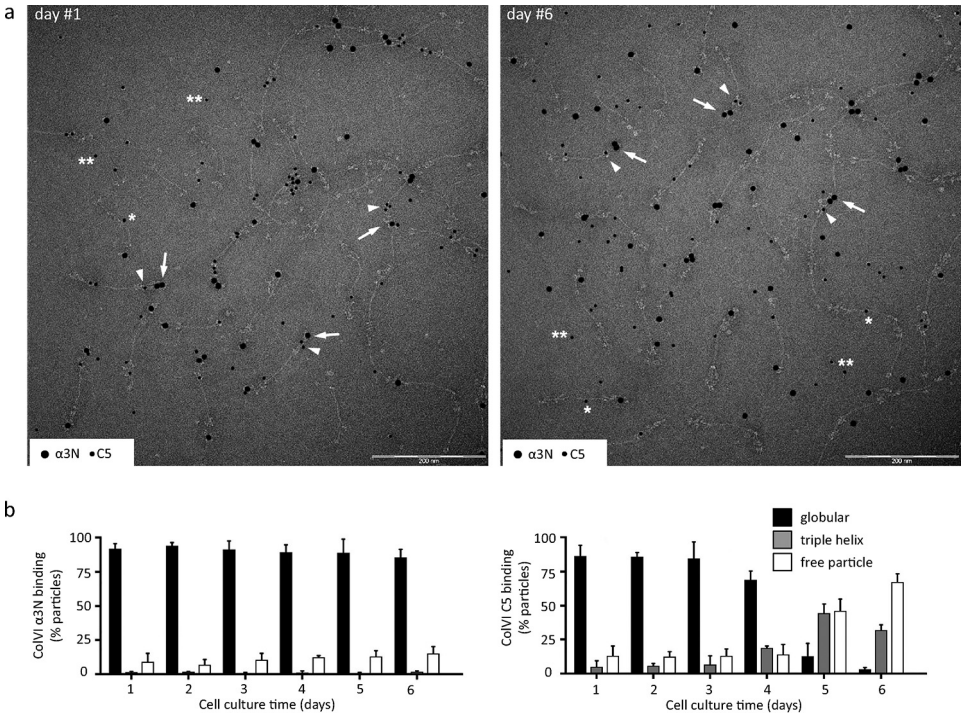

Figure 5. Processing of the C-terminal region of the collagen VI α3 chain occurs after microfibril formation. *a*, representative collagen VI microfibrils in supernatants of primary fibroblast cultures after 1 and 6 days visualized by EM after negative staining and double labeling using gold-labeled affinity-purified antibodies against the N terminus (10 nm; *arrows*) and the C5 domain (5 nm; *arrowheads*) of the collagen VI α3 chain. *Bar*, 200 nm. *Single asterisks* indicate the antibody against the C5 domain binding to the triple-helical region; *double asterisks* indicate antibody binding to C5-containing free particles clearly separated from assembled collagen VI microfibrils. *b*, statistical evaluation of the location of antibody binding. For each time point, 500 particles from randomly selected areas were counted.

for its *in vivo* occurrence as a free fragment, and the protease responsible for its release and the cleavage site have not been identified.

There are conflicting literature data on the presence of the C terminus of the α3 chain as part of the microfibrils. Whereas it was shown by Mayer *et al.* (36) that the extracellular matrix produced by human fibroblasts cannot be stained by an antibody against the C5 domain, Lamande *et al.* (28) described that the extracellular matrix of SaOS-2 cells that express N6-C5 of the α3 chain contains C5 epitopes. The reason for this discrepancy remains unclear. We therefore performed immunoelectron microscopy on microfibrils from cell culture supernatants of primary mouse fibroblasts using gold-labeled antibodies against the C5 domain. Indeed, the gold particles were found at the globular regions of microfibrils, but the epitopes gradually disappeared upon prolonged cell culture. Together with the fact that secreted tetramers still contain C5 epitopes (Fig. 4*b*), this unequivocally shows that the C5 domain is part of freshly formed microfibrils and is cleaved off during fibril maturation. This is in line with the observation that the C5 epitopes are lost with growing distance from chondrocytes (Fig. 1*e*) (23) and could indicate that the relevant protease may act in close vicinity to the plasma membrane.

The composition and fate of the released C-terminal C5-containing fragments remains uncertain. By immunoblotting of cell culture supernatants, body fluids, and tissue extracts, a large variety of fragments were detected. Their apparent molecular masses ranged from 8 up to 120 kDa, but their intensities strongly varied, and fragments corresponding to free endotrophin were hardly detectable by immunoblotting even when

overexposed. Therefore, either the cleaved-off C5 domain (endotrophin) is immediately degraded after cleavage or only a minority of the larger C5-containing fragments are further cleaved. A band that consistently appears, although with different intensities, runs at around 100 kDa upon SDS-PAGE. Interestingly, recombinant C2–C5 runs at this position, although its mass according to sequence is around 70 kDa, indicating an aberrant mobility. This could be caused by post-translational modifications (the repetitive unique domain (C3) contains many predicted *O*-glycosylation sites) or the presence of disordered domains. Interestingly, the murine C3/unique domain has a high proline (23%), alanine (25%), and serine/threonine (10%) content, and it has been shown that proline/alanine and proline/alanine/serine polymers migrate at positions corresponding to much higher molecular masses than expected (37, 38), probably due to reduced binding of SDS. Interestingly, fusion proteins consisting of small proteins and repeats of proline/alanine/serine residues have a drastically increased half-life in serum compared with the small protein alone, most likely because they evade fast clearance from circulation via kidney filtration (38). This could explain why a band corresponding to C2–C5 is found in reasonable amounts in serum. As a variety of larger C5-containing fragments can be extracted from tissue and mature microfibrils do not contain C2–C5 (24), the differential and restricted staining obtained with a C5 antibody points to the deposition of C-terminal fragments in the matrix independent of collagen VI microfibrils. However, their physiological role remains unclear.

Two proteases were identified as being involved in the complex proteolytic processing of the collagen VI α3 chain C terminus: BMP-1 cleaving off the C5 domain (endotrophin) and a proprotein convertase of the furin type cleaving off the large C2–C5 fragment. BMP-1 is a well-known procollagen C-proteinase that is involved in the processing and maturation of the fibrillar collagens I, II, III, V, and XI, but also of other substrates (*e.g.* laminin 332, lysyl oxidases, and small leucine-rich proteoglycans) (39). The new role for BMP-1 as a potential partner in the maturation of collagen VI microfibrils is indeed highly coherent with the previous functions established for the protease in the control of extracellular matrix assembly. Furthermore, the anchoring fibril-forming collagen VII and the follistatin-related protein WFIKKN1 that also contain one or two C-terminal Kunitz domains are cleaved by BMP-1, and fragments containing these domains are released (40, 41). As in the case of collagen VI, the Kunitz domain is necessary for assembly of collagen VII and is cleaved during maturation (42). Contrary to endotrophin, however, there are no reports of an independent role for the cleaved C-terminal Kunitz domain of collagen VII. In the case of WFIKKN1, the prior release of the KKN fragment (containing two Kunitz domains and one NTR domain) strongly increases its capacity to activate the cleavage of myostatin by BMP-1 (41).

Proprotein convertases process and modulate proteins in the secretory compartment, at the plasma membrane, and in the extracellular space (43). A subgroup of seven members cleaves at specific single or paired basic amino acid residues with the consensus motif (R/K)X_n(R/K) ↓ (with n = 0, 2, 4 or 6). The collagen VI α3 chain is indeed cleaved at the perfectly matching RDRR motif (with n = 2) between the C1 and C2 domains, a cleavage that can be suppressed by inhibitors mimicking the consensus site. The physiological relevance of this cleavage is further supported by the fact that the AAGSDVDIDMAFILDSAETTTLFQFNEMK(K) peptide, which defines the N terminus of the released C2–C5 fragment, is listed in the PeptideAtlas Database (44), where it was shown by MS-based approaches to be present in human plasma and ovarian and non-small-cell lung tumor samples. The presence of this peptide in plasma is also coherent with the immunodetection of C2–C5 in mouse serum described in the present study. As tetramers containing the full C terminus are secreted, the proprotein convertase responsible must be located at the plasma membrane (furin, PC5B, PC7, PACE4, and PC5A can be found bound to the cell surface (43)) or in the extracellular compartment (PACE4 and PC5A can be secreted (43)). Although proprotein convertases act as sheddases to release the ectodomains of the transmembrane collagens XIII, XVII, and XXIII and the collagen-like gliomedin (45–48), the extracellular processing of the nontransmembrane collagen VI by a proprotein convertase is unique within the collagen protein family.

Endotrophin function has been studied in mice that lack expression of the collagen VI α1 chain and in mice that overexpress endotrophin (22, 26, 49). However, as shown here, free endotrophin is scarce under physiological conditions compared with the larger endotrophin-containing fragments. Further, the *Col6a1* knockout mice still express and secrete some α3 chain (17). Therefore, the interpretation of data obtained from these mouse models becomes difficult. At present, a mouse model that completely lacks the α3 chain is not available. The hypomorphic *Col6a3*$^{hm/hm}$ mice, with strongly reduced collagen VI expression due to an in-frame deletion of exon 15 of *Col6a3*, lack a severe phenotype (50). This indicates that also a marked reduction of α3 chain expression does not have pronounced effects other than a mild muscular dystrophy similar to that observed in *Col6a1* knockout mice. Also in *Col6a3*$^{+/d16}$ mice, mimicking the most common molecular defect found in dominant Ullrich congenital muscular dystrophy patients, α3 chain–containing tetramers are secreted. Interestingly, in these mice, a reduced processing of the C terminus of the α3 chain is observed (51). However, also here phenotypes other than a collagen VI–related myopathy were not observed. The results may indicate that alterations in the expression of the α3 chain and/or its C-terminal C5-containing fragments may be involved in the pathogenesis of collagen VI–related myopathies but do not have an independent effect if the mice are not in addition challenged (*e.g.* by wounding, high-fat diet, or cancerogenesis). Nevertheless, it is possible that, within the spectrum of collagen VI–related myopathies, the complete lack of the α3 chain or its C-terminal globular domain results in more severe progression. Indeed, a patient who carried a homozygous mutation in an exon coding for the triple-helical part of the α3 chain leading to a stop codon (R2342X) was never able to walk (52). To the best of our knowledge, there are no other patients described who lack expression of the α3 chain or its C-terminal globular domain.

The serum endotrophin level was proposed to serve as a biomarker in certain pathological conditions. An ELISA for endo-

trophin, in this context named Pro-C6, is commercially available (53). Serum Pro-C6 levels can be used to monitor the progression of chronic obstructive pulmonary disease (COPD) (54–57) and systemic sclerosis (58). These are elevated in angina pectoris patients without significant coronary artery disease (59), associated with progression to end-stage renal disease (60), and increased in patients with chronic kidney disease after kidney transplantation (61). Pro-C6 serum levels predict cardiovascular events and disease progression in patients with type 2 diabetes and microalbuminuria (62), and endotrophin is significantly associated with therapeutic response to PPARγ agonists in type 2 diabetes (63). Moreover, urinary endotrophin/creatinine ratio predicts disease progression of chronic kidney disease patients (64). The different Pro-C6–based studies clearly indicate the value of endotrophin as a biomarker. However, due to the much higher abundance of larger endotrophin-containing fragments, it is likely that the Pro-C6 antibody detects a mixture of endotrophin-containing fragments rather than C5 alone. In this context, it is of great interest that the TEPLALTETDICK peptide, which defines the N terminus of the BMP-1–released endotrophin, was previously identified in several human tissues (breast tumors) and body fluids (urine, plasma, and cerebrospinal fluid) according to the PeptideAtlas Database (44). It should therefore be feasible to design a more specific assay to discriminate between the various circulating forms of endotrophin.

In summary, the identification of endotrophin as an adipokine and its use as a disease biomarker encouraged us to study its release and biochemical nature in greater detail. We thereby provide a more solid basis for understanding endotrophin function and information that can be used to refine its use as a biomarker and to unravel the function of the larger C-terminal fragments of the collagen VI α3 chain.

Experimental procedures

Expression and purification of recombinant proteins

BMP-1 was expressed in human embryonic kidney 293-EBNA cells and purified as described previously (65). For expression of the C5 domains of the human (Lys^{3077}–Thr^{3177}; recombinant hC5) and murine (Lys^{3194}–Val^{3284}; recombinant mC5) collagen VI α3 chains, the sequences of the last three exons were chosen. The human endotrophin sequence (Thr^{3101}–Thr^{3177}) was chosen starting at the BMP1 cleavage site. Murine C1–C5 (Leu^{2391}–Val^{3284}) and C2–C5 (Ala^{2608}–Val^{3284}) constructs were also cloned. The human cDNA constructs were generated by PCR on total RNA from placenta and the murine constructs on a plasmid encoding the full C-terminal noncollagenous domains of the α3 chain. The constructs were cloned with 5′-terminal NheI and 3′-terminal BamHI restriction sites using the following primers: hETP (forward), 5′-AAA GCT AGC GAC AGA ACC ATT GGC TCT C-3′; hC5 (forward), 5′-AAA GCT AGC GAA GAA ATC TCA GCC CCC A-3′; hC5 (reverse), 5′-TTT GGA TCC GGT TCC CAT CAC ACT GAT-3′; mC1-C5 (forward), 5′-AAA GCT AGC ACT GGA GTG CCC TGT ATT CCC AAC-3′; mC2-C5 (forward), 5′-AAA GCT AGC AGC AGC AGG CAG TGA T-3′; mC5 (forward), 5′-AAA GCT AGC GAA GAA AAC CCA GCC TCC AC-3′; and the murine reverse primer, 5′-TTT GGA TCC AAC TGT TAA CTC AGG ACT ACA CA-3′. The amplified PCR products were inserted into a modified pCEP-Pu vector containing an N-terminal BM-40 signal peptide and a C-terminal One-STrEP tag downstream of the restriction sites (48). The recombinant plasmids were introduced into 293-EBNA cells (Invitrogen) using the FuGENE 6 transfection reagent (Roche Applied Science). Cells were selected with puromycin (1 μg/ml), and the recombinant proteins were purified directly from serum-free culture medium. After filtration and centrifugation (1 h, 10,000 × *g*), the supernatants were applied to a StrepTactin column (1.5 ml; IBA GmbH) and eluted with 2.5 mM desthiobiotin, 10 mM Tris-HCl, pH 8.0.

Animal experiments

All experiments were approved by the institutional review board "Landesamt für Natur, Umwelt und Verbraucherschutz Nordrhein-Westfalen" (Genehmigung 40.14.065) and performed in accordance with the guidelines of the German animal protection law.

Antibodies

The purified recombinant Strep-tagged murine collagen VI α3 C5 domain (Lys^{3194}–Val^{3284}) and human endotrophin (Thr^{3101}–Thr^{3177}) were used to immunize rabbits (Pineda Antibody Service, Berlin, Germany). The antisera obtained were affinity-purified on a column with the antigen coupled to CNBr-activated Sepharose 4B column (GE Healthcare Life Sciences). The bound antibodies were eluted with 0.1 M glycine, pH 2.5, and the eluate was neutralized with 1 M Tris-HCl, pH 8.8, and adjusted to 150 mM NaCl. The specificity of the purified antibodies was tested by ELISA and immunoblotting (Fig. S1). The generation of the antibody against the N-terminal globular region of the collagen VI α3 chain has been described elsewhere (4).

Immunofluorescence microscopy

Immunofluorescence microscopy was performed on frozen (7 μm) and paraffin-embedded (10 μm) sections of newborn and 8-week-old mice or on cultures of primary dermal fibroblasts grown to confluence on chamber slides. Paraffin-embedded sections were deparaffinized and rehydrated in PBS. Frozen sections were left at room temperature for 1 h, preincubated for 5 min in PBS, fixed with methanol and acetone (1:1) at −20 °C for 10 min, and washed three times with PBS for 5 min. Cells were fixed in 4% paraformaldehyde at room temperature for 10 min. The frozen and deparaffinized sections were incubated with freshly dissolved bovine testicular hyaluronidase (50 units/ml) for 30 min at 37 °C, washed twice with Tris-buffered saline (TBS) for 5 min each, treated 10 min with 0.2% Triton X-100/TBS, and washed twice with TBS for 5 min each before the sections were blocked for 1 h with 1% BSA/TBS at room temperature. The primary antibodies were diluted in 1% BSA/TBS for use on tissue sections or 1% BSA/PBS for use on cells, applied to sections or cell monolayers for 1 h at room temperature before washing three times for 5 min with 0.05% Tween 20/TBS or PBS, respectively. Subsequently, sections and cells were incubated with either Alexa Fluor 488–conjugated goat

anti-rabbit IgG (Thermo Fisher Scientific), Cy3-conjugated goat anti-guinea pig IgG (Dianova), or Alexa Fluor 555 donkey anti-rabbit IgG (Thermo Fisher Scientific) for 1 h in the dark, washed three times with TBS, and mounted with DAKO fluorescent mounting medium.

Tissue extraction

Tissues of newborn and 8-week-old C57/Bl6 mice were shock-frozen in liquid nitrogen; ground with pestle and mortar; incubated with 1 mM Tris, pH 7.4, containing 750 mM NaCl, 5% Nonidet P-40, 0.25% Triton X-100, 2.5% SDS, 2.5 mM EDTA, and protease inhibitors (Complete, Roche Applied Science) for 30 min on ice; and centrifuged at 4 °C for 10 min.

SDS-PAGE and immunoblotting

Samples for SDS-PAGE were subjected to electrophoresis on a 4–12% Tris-glycine gradient, precast 4–20% TGX (Bio-Rad), or precast 12% BisTris polyacrylamide gels (Thermo Fisher Scientific). For agarose/polyacrylamide composite gel electrophoresis, samples were supplemented with SDS-sample buffer and urea (final concentration of 2 M) and subjected to electrophoresis on 0.5% (w/v) agarose, 2.4% (w/v) polyacrylamide composite gels. For immunoblotting, the proteins were transferred either onto a polyvinylidene fluoride (0.2 μm; Thermo Fisher Scientific or Millipore) or nitrocellulose (0.2 μm; GE Healthcare) membrane. Membranes were blocked with 5% milk powder in 0.05% Tween 20/TBS, incubated with the primary antibody and secondary horseradish peroxidase–conjugated polyclonal donkey anti-rabbit IgG (DAKO or Cell Signaling Technology) diluted in 5% milk powder/TBS, 0.05% Tween 20. Signals were detected by chemiluminescence (ECL).

Fibroblast culture and furin inhibition

Primary dermal fibroblasts were freshly isolated from newborn mice (postnatal days 0–2). Cells were grown in Dulbecco's modified Eagle's medium (DMEM GlutaMAX, Invitrogen) supplemented with 10% FCS and penicillin/streptomycin on uncoated glass coverslips at a density of 8×10^4 cells/well in a 24-well plate and supplemented every second day with ascorbic acid (0.125 mM ascorbate, 0.225 mM L-ascorbic acid 2-phosphate). For inhibition of the proprotein convertase furin, cells were grown to confluence, washed with PBS, and cultured in the presence of 0.1% FCS for 10 h. Subsequently, the cells were incubated in the presence of 0.1% FCS supplemented with 5, 15, or 30 μM furin inhibitor I (Merck Millipore) or only DMSO. The media were harvested after 48 h and subjected to SDS-PAGE.

Keratocyte culture

Human primary keratocytes were isolated from human corneas rejected for clinical use and harvested at the Cell and Tissue Bank of the "Hospices Civils de Lyon." Cell harvesting was approved by the French Research Ministry (authorization no. AC 2013-1846). Informed consent was obtained from the donors' families after verification of the National Register of organ donation refusal, and the study conformed to the standards of the Declaration of Helsinki. Keratocytes were used as a pool of three donors (aged around 70). Keratocytes were grown in DMEM/Ham's F-12 (1:1), 10% iron-supplemented newborn bovine serum (Hyclone, Fisher Scientific), 1% antibiotic/antimycotic solution (Sigma-Aldrich), and 5 ng/ml basic fibroblast growth factor (Sigma-Aldrich) (66). When reaching 90% confluence, cells were incubated with phenol red–free, serum-free DMEM supplemented with 2 mM glutamine and 1% antibiotic/antimycotic solution. The medium was harvested after 48 h. Protease inhibitors were immediately added (10 μM E64, 15 μM GM6001, and 0.25 mM AEBSF), and the medium was clarified by centrifugation (200 × g, 10 min) and filtration (Steriflip, Millipore), concentrated with ultrafiltration devices (Centricon-Plus 70 with 10-kDa molecular weight cutoff; Millipore), and stored at −80 °C.

BMP-1 cleavage assay

Cleavage assays involving recombinant C5 domain constructs were performed in 50 mM HEPES, pH 7.4, 0.22 M NaCl, 5 mM $CaCl_2$, and 0.04% octyl-β,D-glucopyranoside in a total volume of 200 μl at 37 °C for 4 h. Protease/substrate molar ratios of between 1:1 and 1:150 were used, and detection was by SDS-PAGE on 15% Tris-glycine polyacrylamide gels with Coomassie Blue staining or ATOMS. When concentrated keratocyte medium was used as a source of substrates, between 27 and 200 μg of total protein (assessed with the Bradford assay) were incubated with BMP-1 (1:50 or 1:100 protease/total protein ratio) or 10 μM BMP-1 hydroxamate inhibitor (S33A) (67) in 20 mM HEPES, pH 7.4, 0.15 M NaCl, 5 mM $CaCl_2$, and 0.05% octyl-β,D-glucopyranoside for 2–4 h at 37 °C. Analysis was by Western blotting with an antibody against human C5 domain or TAILS.

Sample preparation for TAILS and ATOMS experiments

For TAILS experiments, keratocytes were maintained in serum-free medium for 48 h in the presence of 10 μM S33A inhibitor or vehicle (1% DMSO). The harvested keratocyte supernatants were clarified, concentrated as above, and analyzed in a 4-plex format: condition 1, concentrated medium treated with S33A; condition 2, concentrated medium treated with DMSO; condition 3, concentrated medium treated with DMSO and incubated with 10 μM S33A for 4 h at 37 °C; condition 4, concentrated medium treated with DMSO and incubated with recombinant BMP-1 (1:50 protease/total protein ratio) for 4 h at 37 °C.

The four samples were then processed as described previously (30, 68) with minor modifications. Samples were first precipitated with 15% TCA at 4 °C for 4 h, and after four washes in cold acetone, the pellet was dissolved in 250 mM HEPES, pH 8, and 2.5 M guanidinium chloride. The samples were then denaturated at 65 °C for 15 min, reduced in the presence of 1 mM tris(2-carboxyethyl) phosphine for 45 min at 65 °C, and alkylated with 5 mM iodoacetamide for 45 min at room temperature. iTRAQ labels (113–116; iTRAQ 8-plex kit from ABSciex) were dissolved in DMSO and added in a 1:5 (total protein/iTRAQ label) mass ratio to one of the four samples (200 μg of total protein/condition) for 30 min. Labeling reactions were quenched with 100 mM ammonium bicarbonate for 30 min, and the four samples were mixed and precipitated with cold methanol/acetone (8:1) (v/v). After two washes with cold methanol,

the pellet was resuspended in 100 mM HEPES, pH 8, to obtain a final protein concentration of 2 mg/ml and submitted to overnight trypsin digestion (trypsin/total protein (1:20); Trypsin Gold, Promega). The digested sample was then enriched in N-terminal peptides through removal of internal tryptic peptides with a 1:5 mass excess of dialyzed HPG-ALD polymer (30) and desalted with a C18 spin column (Thermo Fisher Scientific). The eluate fraction was freeze-dried and resuspended in 0.1% TFA.

For ATOMS experiments (31, 32), 10 μg of the mouse recombinant mC5 domain was incubated either with recombinant BMP-1 or buffer under the conditions described above (protease/substrate molar ratio of 1:30 for 4 h). Sample denaturation, reduction, alkylation, labeling, precipitation, digestion with trypsin, and desalting was performed exactly as for TAILS samples. The initial precipitation with TCA and the negative selection step with the HPG-ALD polymer were left out.

Mass spectrometry

LC-MS/MS experiments were performed on a Q-Exactive HF mass spectrometer operated with the Xcalibur software (version 4.0) and equipped with an RSLC Ultimate 3000 nano-LC system (Thermo Scientific). A C_{18} column (Acclaim Pepmap, 75-μm inner diameter $\times$ 50 cm; 100-Å pore and 3-μm particle size) was coupled in line to the mass spectrometer to resolve peptides before nanospray injection into the mass spectrometer. For this, a 180-min linear gradient of acetonitrile, 0.1% formic acid was applied from 4 to 40% acetonitrile at 300 nl/min. The Q-Exactive HF instrument was operated according to a Top20 data-dependent method consisting of a scan cycle initiated with a full scan of peptide ions in the ultra-high-field Orbitrap analyzer, followed by selection of the precursor with a fixed first mass parameter set at 80 m/z and high-energy collisional dissociation with a normalized energy collision fixed at 33 eV. MS/MS scans were recorded at a resolution of 15,000 on the 20 most abundant precursor ions with an automatic gain control (AGC) target set at 10^5 ions with a threshold intensity of 10^5 and a dynamic exclusion of 10 s. Only ions with potential charge states of 2+ and 3+ were selected. MS spectra on precursors were acquired at a resolution of 60,000 from m/z 350 to 1,800 when the AGC target reached 3×10^6 ions.

Peak lists (.mgf files) were generated with the Trans-Proteomic Pipeline (TPP) version 5.0 (69) and used for database searches with MASCOT 2.4.1. Mass spectrometry data were searched against the human Swiss-Prot database (release 2017_03, 40,500 entries including reversed decoy sequences and, for ATOMS experiments, the sequences of the relevant recombinant proteins) with a mass tolerance of 10 ppm for precursor and 0.02 Da for fragment ions. Cysteine carbamidomethyl was set as a fixed modification; methionine oxidation, N-terminal acetylation, proline hydroxylation, and iTRAQ labeling of the N terminus and lysines were considered as variable modifications. Two missed cleavages were allowed, and trypsin cleavage specificity was selected. A secondary peptide and protein validation was achieved with the TPP, as described previously (31). Quantitation was achieved using the LIBRA tool of the TPP (default parameters), and ratios corresponding to condition 2/condition 1 (DMSO/inhibitor in cell culture) and condition 4/condition 1 (BMP-1/inhibitor *in vitro*) were calculated. The final protein lists were compiled using ProteinProphet with a probability of 0.75 resulting in low error rates of 5%.

EM

Proteolytic processing of the collagen VI α3 chain in the supernatant of primary dermal mouse fibroblast cultures (1–6-day cultivation time) was analyzed by incubation for 30 min at 37 °C with 5- and 10-nm colloidal gold-labeled (70) antibodies specific for the N-terminal regions and the C5 domain of collagen VI α3 chain followed by negative staining and transmission EM as described (71). Specimens were observed in a Philips/FEICM 100 TWIN transmission electron microscope operated at 60-kV accelerating voltage. Images were recorded with a side-mounted Olympus Veleta camera with a resolution of 2048 $\times$ 2048 pixels and the ITEM acquisitions software.

Author contributions—S. E. H., M. T., M. N., J. A., M. M., and U. H. investigation; S. E. H., M. T., M. N., J. A., M. M., U. H., G. S., M. P., C. M., and R. W. methodology; G. S., M. P., C. M., and R. W. supervision; G. S., M. P., C. M., and R. W. funding acquisition; M. P., C. M., and R. W. writing-original draft; C. M. and R. W. conceptualization; C. M. and R. W. project administration.

Acknowledgments—We are grateful to the staff in the BioEM laboratory, Biozentrum, University of Basel, the microscopy facility at the Department of Biology, Lund University, and the Core Facility for Integrated Microscopy (CFIM), Panum Institute, University of Copenhagen, for providing highly innovative environments for EM. We thank Cinzia Tiberi (BioEM laboratory) and Ola Gustafsson (microscopy facility) for skillful work; Carola Alampi (BioEM laboratory), Mohamed Chami (BioEM laboratory), and Klaus Qvortrup (CFIM) for practical help with EM; Johanna Hülsmann (Center for Biochemistry, Medical Faculty, University of Cologne) for technical assistance; and Frédéric Delolme (Protein Science Facility, SFR Biosciences, UMS3444 CNRS/US8 INSERM/ENS Lyon/University of Lyon) for help with the MS analyses.

References

1. Cescon, M., Gattazzo, F., Chen, P., and Bonaldo, P. (2015) Collagen VI at a glance. *J. Cell Sci.* **128,** 3525–3531 CrossRef Medline
2. Gara, S. K., Grumati, P., Urciuolo, A., Bonaldo, P., Kobbe, B., Koch, M., Paulsson, M., and Wagener, R. (2008) Three novel collagen VI chains with high homology to the α3 chain. *J. Biol. Chem.* **283,** 10658–10670 CrossRef Medline
3. Fitzgerald, J., Rich, C., Zhou, F. H., and Hansen, U. (2008) Three novel collagen VI chains, α4(VI), α5(VI), and α6(VI). *J. Biol. Chem.* **283,** 20170–20180 CrossRef Medline
4. Maass, T., Bayley, C. P., Mörgelin, M., Lettmann, S., Bonaldo, P., Paulsson, M., Baldock, C., and Wagener, R. (2016) Heterogeneity of collagen VI microfibrils: structural analysis of non-collagenous regions. *J. Biol. Chem.* **291,** 5247–5258 CrossRef Medline
5. Gara, S. K., Grumati, P., Squarzoni, S., Sabatelli, P., Urciuolo, A., Bonaldo, P., Paulsson, M., and Wagener, R. (2011) Differential and restricted expression of novel collagen VI chains in mouse. *Matrix Biol.* **30,** 248–257 CrossRef Medline
6. Wagener, R., Gara, S. K., Kobbe, B., Paulsson, M., and Zaucke, F. (2009) The knee osteoarthritis susceptibility locus DVWA on chromosome 3p24.3 is the 5′ part of the split COL6A4 gene. *Matrix Biol.* **28,** 307–310 CrossRef Medline

7. Bonaldo, P., Braghetta, P., Zanetti, M., Piccolo, S., Volpin, D., and Bressan, G. M. (1998) Collagen VI deficiency induces early onset myopathy in the mouse: an animal model for Bethlem myopathy. *Hum. Mol. Genet.* **7,** 2135–2140 CrossRef Medline
8. Irwin, W. A., Bergamin, N., Sabatelli, P., Reggiani, C., Megighian, A., Merlini, L., Braghetta, P., Columbaro, M., Volpin, D., Bressan, G. M., Bernardi, P., and Bonaldo, P. (2003) Mitochondrial dysfunction and apoptosis in myopathic mice with collagen VI deficiency. *Nat. Genet.* **35,** 367–371 CrossRef Medline
9. Grumati, P., Coletto, L., Sabatelli, P., Cescon, M., Angelin, A., Bertaggia, E., Blaauw, B., Urciuolo, A., Tiepolo, T., Merlini, L., Maraldi, N. M., Bernardi, P., Sandri, M., and Bonaldo, P. (2010) Autophagy is defective in collagen VI muscular dystrophies, and its reactivation rescues myofiber degeneration. *Nat. Med.* **16,** 1313–1320 CrossRef Medline
10. Cescon, M., Gregorio, I., Eiber, N., Borgia, D., Fusto, A., Sabatelli, P., Scorzeto, M., Megighian, A., Pegoraro, E., Hashemolhosseini, S., and Bonaldo, P. (2018) Collagen VI is required for the structural and functional integrity of the neuromuscular junction. *Acta Neuropathol.* **136,** 483–499 CrossRef Medline
11. Cheng, J. S., Dubal, D. B., Kim, D. H., Legleiter, J., Cheng, I. H., Yu, G. Q., Tesseur, I., Wyss-Coray, T., Bonaldo, P., and Mucke, L. (2009) Collagen VI protects neurons against Aβ toxicity. *Nat. Neurosci.* **12,** 119–121 CrossRef Medline
12. Chen, P., Cescon, M., Megighian, A., and Bonaldo, P. (2014) Collagen VI regulates peripheral nerve myelination and function. *FASEB J.* **28,** 1145–1156 CrossRef Medline
13. Chen, P., Cescon, M., Zuccolotto, G., Nobbio, L., Colombelli, C., Filaferro, M., Vitale, G., Feltri, M. L., and Bonaldo, P. (2015) Collagen VI regulates peripheral nerve regeneration by modulating macrophage recruitment and polarization. *Acta Neuropathol.* **129,** 97–113 CrossRef Medline
14. Alexopoulos, L. G., Youn, I., Bonaldo, P., and Guilak, F. (2009) Developmental and osteoarthritic changes in Col6a1-knockout mice: biomechanics of type VI collagen in the cartilage pericellular matrix. *Arthritis Rheum.* **60,** 771–779 CrossRef Medline
15. Christensen, S. E., Coles, J. M., Zelenski, N. A., Furman, B. D., Leddy, H. A., Zauscher, S., Bonaldo, P., and Guilak, F. (2012) Altered trabecular bone structure and delayed cartilage degeneration in the knees of collagen VI null mice. *PLoS One* **7,** e33397 CrossRef Medline
16. Izu, Y., Ezura, Y., Mizoguchi, F., Kawamata, A., Nakamoto, T., Nakashima, K., Hayata, T., Hemmi, H., Bonaldo, P., and Noda, M. (2012) Type VI collagen deficiency induces osteopenia with distortion of osteoblastic cell morphology. *Tissue Cell* **44,** 1–6 CrossRef Medline
17. Lettmann, S., Bloch, W., Maass, T., Niehoff, A., Schulz, J. N., Eckes, B., Eming, S. A., Bonaldo, P., Paulsson, M., and Wagener, R. (2014) Col6a1 null mice as a model to study skin phenotypes in patients with collagen VI related myopathies: expression of classical and novel collagen VI variants during wound healing. *PLoS One* **9,** e105686 CrossRef Medline
18. Chen, P., Cescon, M., and Bonaldo, P. (2015) Lack of collagen VI promotes wound-induced hair growth. *J. Invest. Dermatol.* **135,** 2358–2367 CrossRef Medline
19. Luther, D. J., Thodeti, C. K., Shamhart, P. E., Adapala, R. K., Hodnichak, C., Weihrauch, D., Bonaldo, P., Chilian, W. M., and Meszaros, J. G. (2012) Absence of type VI collagen paradoxically improves cardiac function, structure, and remodeling after myocardial infarction. *Circ. Res.* **110,** 851–856 CrossRef Medline
20. Izu, Y., Ansorge, H. L., Zhang, G., Soslowsky, L. J., Bonaldo, P., Chu, M. L., and Birk, D. E. (2011) Dysfunctional tendon collagen fibrillogenesis in collagen VI null mice. *Matrix Biol.* **30,** 53–61 CrossRef Medline
21. Dassah, M., Almeida, D., Hahn, R., Bonaldo, P., Worgall, S., and Hajjar, K. A. (2014) Annexin A2 mediates secretion of collagen VI, pulmonary elasticity and apoptosis of bronchial epithelial cells. *J. Cell Sci.* **127,** 828–844 CrossRef Medline
22. Park, J., and Scherer, P. E. (2012) Adipocyte-derived endotrophin promotes malignant tumor progression. *J. Clin. Invest.* **122,** 4243–4256 CrossRef Medline
23. Aigner, T., Hambach, L., Söder, S., Schlötzer-Schrehardt, U., and Pöschl, E. (2002) The C5 domain of Col6A3 is cleaved off from the Col6 fibrils immediately after secretion. *Biochem. Biophys. Res. Commun.* **290,** 743–748 CrossRef Medline
24. Beecher, N., Roseman, A. M., Jowitt, T. A., Berry, R., Troilo, H., Kammerer, R. A., Shuttleworth, C. A., Kielty, C. M., and Baldock, C. (2011) Collagen VI, conformation of A-domain arrays and microfibril architecture. *J. Biol. Chem.* **286,** 40266–40275 CrossRef Medline
25. Fitzgerald, J., Mörgelin, M., Selan, C., Wiberg, C., Keene, D. R., Lamandé, S. R., and Bateman, J. F. (2001) The N-terminal N5 subdomain of the α3(VI) chain is important for collagen VI microfibril formation. *J. Biol. Chem.* **276,** 187–193 CrossRef Medline
26. Sun, K., Park, J., Gupta, O. T., Holland, W. L., Auerbach, P., Zhang, N., Goncalves Marangoni, R., Nicoloro, S. M., Czech, M. P., Varga, J., Ploug, T., An, Z., and Scherer, P. E. (2014) Endotrophin triggers adipose tissue fibrosis and metabolic dysfunction. *Nat. Commun.* **5,** 3485 CrossRef Medline
27. Park, J., Morley, T. S., and Scherer, P. E. (2013) Inhibition of endotrophin, a cleavage product of collagen VI, confers cisplatin sensitivity to tumours. *EMBO Mol. Med.* **5,** 935–948 CrossRef Medline
28. Lamandé, S. R., Mörgelin, M., Adams, N. E., Selan, C., and Allen, J. M. (2006) The C5 domain of the collagen VI α3(VI) chain is critical for extracellular microfibril formation and is present in the extracellular matrix of cultured cells. *J. Biol. Chem.* **281,** 16607–16614 CrossRef Medline
29. Nanda, A., Carson-Walter, E. B., Seaman, S., Barber, T. D., Stampfl, J., Singh, S., Vogelstein, B., Kinzler, K. W., and St Croix, B. (2004) TEM8 interacts with the cleaved C5 domain of collagen α3(VI). *Cancer Res.* **64,** 817–820 CrossRef Medline
30. Kleifeld, O., Doucet, A., auf dem Keller, U., Prudova, A., Schilling, O., Kainthan, R. K., Starr, A. E., Foster, L. J., Kizhakkedathu, J. N., and Overall, C. M. (2010) Isotopic labeling of terminal amines in complex samples identifies protein N-termini and protease cleavage products. *Nat. Biotechnol.* **28,** 281–288 CrossRef Medline
31. Delolme, F., Anastasi, C., Alcaraz, L. B., Mendoza, V., Vadon-Le Goff, S., Talantikite, M., Capomaccio, R., Mevaere, J., Fortin, L., Mazzocut, D., Damour, O., Zanella-Cléon, I., Hulmes, D. J., Overall, C. M., Valcourt, U., Lopez-Casillas, F., and Moali, C. (2015) Proteolytic control of TGF-β coreceptor activity by BMP-1/tolloid-like proteases revealed by quantitative iTRAQ proteomics. *Cell Mol. Life Sci.* **72,** 1009–1027 CrossRef Medline
32. Doucet, A., and Overall, C. M. (2011) Broad coverage identification of multiple proteolytic cleavage site sequences in complex high molecular weight proteins using quantitative proteomics as a complement to edman sequencing. *Mol. Cell. Proteomics* **10,** M110.003533 CrossRef Medline
33. Imamura, Y., Steiglitz, B. M., and Greenspan, D. S. (1998) Bone morphogenetic protein-1 processes the NH_2-terminal propeptide, and a furin-like proprotein convertase processes the COOH-terminal propeptide of pro-α1(V) collagen. *J. Biol. Chem.* **273,** 27511–27517 CrossRef Medline
34. Pappano, W. N., Steiglitz, B. M., Scott, I. C., Keene, D. R., and Greenspan, D. S. (2003) Use of Bmp1/Tll1 doubly homozygous null mice and proteomics to identify and validate *in vivo* substrates of bone morphogenetic protein 1/tolloid-like metalloproteinases. *Mol. Cell. Biol.* **23,** 4428–4438 CrossRef Medline
35. Kim, B., Huang, G., Ho, W. B., and Greenspan, D. S. (2011) Bone morphogenetic protein-1 processes insulin-like growth factor-binding protein 3. *J. Biol. Chem.* **286,** 29014–29025 CrossRef Medline
36. Mayer, U., Pöschl, E., Nischt, R., Specks, U., Pan, T. C., Chu, M. L., and Timpl, R. (1994) Recombinant expression and properties of the Kunitz-type protease-inhibitor module from human type VI collagen α3(VI) chain. *Eur. J. Biochem.* **225,** 573–580 CrossRef Medline
37. Breibeck, J., and Skerra, A. (2018) The polypeptide biophysics of proline/alanine-rich sequences (PAS): recombinant biopolymers with PEG-like properties. *Biopolymers* **109,** 10.1002/bip.23069 CrossRef Medline
38. Schlapschy, M., Binder, U., Börger, C., Theobald, I., Wachinger, K., Kisling, S., Haller, D., and Skerra, A. (2013) PASylation: a biological alternative to PEGylation for extending the plasma half-life of pharmaceutically active proteins. *Protein Eng. Des. Sel.* **26,** 489–501 CrossRef Medline
39. Vadon-Le Goff, S., Hulmes, D. J., and Moali, C. (2015) BMP-1/tolloid-like proteinases synchronize matrix assembly with growth factor activation to promote morphogenesis and tissue remodeling. *Matrix Biol.* **44,** 14–23 CrossRef Medline

40. Rattenholl, A., Pappano, W. N., Koch, M., Keene, D. R., Kadler, K. E., Sasaki, T., Timpl, R., Burgeson, R. E., Greenspan, D. S., and Bruckner-Tuderman, L. (2002) Proteinases of the bone morphogenetic protein-1 family convert procollagen VII to mature anchoring fibril collagen. *J. Biol. Chem.* **277,** 26372–26378 CrossRef Medline
41. Szláma, G., Vásárhelyi, V., Trexler, M., and Patthy, L. (2016) Influence of WFIKKN1 on BMP1-mediated activation of latent myostatin. *FEBS J.* **283,** 4515–4527 CrossRef Medline
42. Colombo, M., Brittingham, R. J., Klement, J. F., Majsterek, I., Birk, D. E., Uitto, J., and Fertala, A. (2003) Procollagen VII self-assembly depends on site-specific interactions and is promoted by cleavage of the NC2 domain with procollagen C-proteinase. *Biochemistry* **42,** 11434–11442 CrossRef Medline
43. Seidah, N. G., and Prat, A. (2012) The biology and therapeutic targeting of the proprotein convertases. *Nat. Rev. Drug Discov.* **11,** 367–383 CrossRef Medline
44. Desiere, F., Deutsch, E. W., King, N. L., Nesvizhskii, A. I., Mallick, P., Eng, J., Chen, S., Eddes, J., Loevenich, S. N., and Aebersold, R. (2006) The PeptideAtlas project. *Nucleic Acids Res.* **34,** D655–D658 CrossRef Medline
45. Snellman, A., Tu, H., Väisänen, T., Kvist, A. P., Huhtala, P., and Pihlajaniemi, T. (2000) A short sequence in the N-terminal region is required for the trimerization of type XIII collagen and is conserved in other collagenous transmembrane proteins. *EMBO J.* **19,** 5051–5059 CrossRef Medline
46. Schäcke, H., Schumann, H., Hammami-Hauasli, N., Raghunath, M., and Bruckner-Tuderman, L. (1998) Two forms of collagen XVII in keratinocytes: a full-length transmembrane protein and a soluble ectodomain. *J. Biol. Chem.* **273,** 25937–25943 CrossRef Medline
47. Veit, G., Zimina, E. P., Franzke, C. W., Kutsch, S., Siebolds, U., Gordon, M. K., Bruckner-Tuderman, L., and Koch, M. (2007) Shedding of collagen XXIII is mediated by furin and depends on the plasma membrane microenvironment. *J. Biol. Chem.* **282,** 27424–27435 CrossRef Medline
48. Maertens, B., Hopkins, D., Franzke, C. W., Keene, D. R., Bruckner-Tuderman, L., Greenspan, D. S., and Koch, M. (2007) Cleavage and oligomerization of gliomedin, a transmembrane collagen required for node of ranvier formation. *J. Biol. Chem.* **282,** 10647–10659 CrossRef Medline
49. Lee, C., Kim, M., Lee, J. H., Oh, J., Shin, H. H., Lee, S. M., Scherer, P. E., Kwon, H. M., Choi, J. H., and Park, J. (2019) COL6A3-derived endotrophin links reciprocal interactions among hepatic cells in the pathology of chronic liver disease. *J. Pathol.* **247,** 99–109 CrossRef Medline
50. Pan, T. C., Zhang, R. Z., Markova, D., Arita, M., Zhang, Y., Bogdanovich, S., Khurana, T. S., Bönnemann, C. G., Birk, D. E., and Chu, M. L. (2013) COL6A3 protein deficiency in mice leads to muscle and tendon defects similar to human collagen VI congenital muscular dystrophy. *J. Biol. Chem.* **288,** 14320–14331 CrossRef Medline
51. Pan, T. C., Zhang, R. Z., Arita, M., Bogdanovich, S., Adams, S. M., Gara, S. K., Wagener, R., Khurana, T. S., Birk, D. E., and Chu, M. L. (2014) A mouse model for dominant collagen VI disorders: heterozygous deletion of Col6a3 Exon 16. *J. Biol. Chem.* **289,** 10293–10307 CrossRef Medline
52. Demir, E., Sabatelli, P., Allamand, V., Ferreiro, A., Moghadaszadeh, B., Makrelouf, M., Topaloglu, H., Echenne, B., Merlini, L., and Guicheney, P. (2002) Mutations in COL6A3 cause severe and mild phenotypes of Ullrich congenital muscular dystrophy. *Am. J. Hum. Genet.* **70,** 1446–1458 CrossRef Medline
53. Sun, S., Henriksen, K., Karsdal, M. A., Byrjalsen, I., Rittweger, J., Armbrecht, G., Belavy, D. L., Felsenberg, D., and Nedergaard, A. F. (2015) Collagen type III and VI turnover in response to long-term immobilization. *PLoS One* **10,** e0144525 CrossRef Medline
54. Stolz, D., Leeming, D. J., Kristensen, J. H. E., Karsdal, M. A., Boersma, W., Louis, R., Milenkovic, B., Kostikas, K., Blasi, F., Aerts, J., Sand, J. M. B., Wouters, E. F. M., Rohde, G., Prat, C., Torres, A., *et al.* (2017) Systemic biomarkers of collagen and elastin turnover are associated with clinically relevant outcomes in COPD. *Chest* **151,** 47–59 CrossRef Medline
55. Bihlet, A. R., Karsdal, M. A., Sand, J. M., Leeming, D. J., Roberts, M., White, W., and Bowler, R. (2017) Biomarkers of extracellular matrix turnover are associated with emphysema and eosinophilic-bronchitis in COPD. *Respir. Res.* **18,** 22 CrossRef Medline
56. Sand, J. M., Martinez, G., Midjord, A. K., Karsdal, M. A., Leeming, D. J., and Lange, P. (2016) Characterization of serological neo-epitope biomarkers reflecting collagen remodeling in clinically stable chronic obstructive pulmonary disease. *Clin. Biochem.* **49,** 1144–1151 CrossRef Medline
57. Sand, J. M., Knox, A. J., Lange, P., Sun, S., Kristensen, J. H., Leeming, D. J., Karsdal, M. A., Bolton, C. E., and Johnson, S. R. (2015) Accelerated extracellular matrix turnover during exacerbations of COPD. *Respir. Res.* **16,** 69 CrossRef Medline
58. Juhl, P., Bay-Jensen, A. C., Karsdal, M., Siebuhr, A. S., Franchimont, N., and Chavez, J. (2018) Serum biomarkers of collagen turnover as potential diagnostic tools in diffuse systemic sclerosis: a cross-sectional study. *PLoS One* **13,** e0207324 CrossRef Medline
59. Nielsen, S. H., Mygind, N. D., Michelsen, M. M., Bechsgaard, D. F., Suhrs, H. E., Genovese, F., Nielsen, H. B., Brix, S., Karsdal, M., Prescott, E., and Kastrup, J. (2018) Accelerated collagen turnover in women with angina pectoris without obstructive coronary artery disease: an iPOWER substudy. *Eur. J. Prev. Cardiol.* **25,** 719–727 CrossRef Medline
60. Fenton, A., Jesky, M. D., Ferro, C. J., Sørensen, J., Karsdal, M. A., Cockwell, P., and Genovese, F. (2017) Serum endotrophin, a type VI collagen cleavage product, is associated with increased mortality in chronic kidney disease. *PLoS One* **12,** e0175200 CrossRef Medline
61. Stribos, E. G. D., Nielsen, S. H., Brix, S., Karsdal, M. A., Seelen, M. A., van Goor, H., Bakker, S. J. L., Olinga, P., Mutsaers, H. A. M., and Genovese, F. (2017) Non-invasive quantification of collagen turnover in renal transplant recipients. *PLoS One* **12,** e0175898 CrossRef Medline
62. Rasmussen, D. G. K., Hansen, T. W., von Scholten, B. J., Nielsen, S. H., Reinhard, H., Parving, H. H., Tepel, M., Karsdal, M. A., Jacobsen, P. K., Genovese, F., and Rossing, P. (2018) Higher collagen VI formation is associated with all-cause mortality in patients with type 2 diabetes and microalbuminuria. *Diabetes Care* **41,** 1493–1500 CrossRef Medline
63. Karsdal, M. A., Henriksen, K., Genovese, F., Leeming, D. J., Nielsen, M. J., Riis, B. J., Christiansen, C., Byrjalsen, I., and Schuppan, D. (2017) Serum endotrophin identifies optimal responders to PPARγ agonists in type 2 diabetes. *Diabetologia* **60,** 50–59 CrossRef Medline
64. Rasmussen, D. G. K., Fenton, A., Jesky, M., Ferro, C., Boor, P., Tepel, M., Karsdal, M. A., Genovese, F., and Cockwell, P. (2017) Urinary endotrophin predicts disease progression in patients with chronic kidney disease. *Sci. Rep.* **7,** 17328 CrossRef Medline
65. Hung, C. W., Koudelka, T., Anastasi, C., Becker, A., Moali, C., and Tholey, A. (2016) Characterization of post-translational modifications in full-length human BMP-1 confirms the presence of a rare vicinal disulfide linkage in the catalytic domain and highlights novel features of the EGF domain. *J. Proteomics* **138,** 136–145 CrossRef Medline
66. Builles, N., Bechetoille, N., Justin, V., Ducerf, A., Auxenfans, C., Burillon, C., Sergent, M., and Damour, O. (2006) Development of an optimised culture medium for keratocytes in monolayer. *Biomed. Mater. Eng.* **16,** S95–S104 Medline
67. Talantikite, M., Lécorché, P., Beau, F., Damour, O., Becker-Pauly, C., Ho, W. B., Dive, V., Vadon-Le Goff, S., and Moali, C. (2018) Inhibitors of BMP-1/tolloid-like proteinases: efficacy, selectivity and cellular toxicity. *FEBS Open Bio.* **8,** 2011–2021 CrossRef Medline
68. Bekhouche, M., Leduc, C., Dupont, L., Janssen, L., Delolme, F., Vadon-Le Goff, S., Smargiasso, N., Baiwir, D., Mazzucchelli, G., Zanella-Cleon, I., Dubail, J., De Pauw, E., Nusgens, B., Hulmes, D. J., Moali, C., and Colige, A. (2016) Determination of the substrate repertoire of ADAMTS2, 3, and 14 significantly broadens their functions and identifies extracellular matrix organization and TGF-β signaling as primary targets. *FASEB J.* **30,** 1741–1756 CrossRef Medline
69. Deutsch, E. W., Mendoza, L., Shteynberg, D., Farrah, T., Lam, H., Tasman, N., Sun, Z., Nilsson, E., Pratt, B., Prazen, B., Eng, J. K., Martin, D. B., Nesvizhskii, A. I., and Aebersold, R. (2010) A guided tour of the Trans-Proteomic Pipeline. *Proteomics* **10,** 1150–1159 CrossRef Medline
70. Baschong, W., and Wrigley, N. G. (1990) Small colloidal gold conjugated to Fab fragments or to immunoglobulin G as high-resolution labels for electron microscopy: a technical overview. *J. Electron Microsc. Tech.* **14,** 313–323 CrossRef Medline
71. Roth, J., Bendayan, M., and Orci, L. (1980) FITC-protein A-gold complex for light and electron microscopic immunocytochemistry. *J. Histochem. Cytochem.* **28,** 55–57 CrossRef Medline

C-terminal proteolysis of the collagen VI α3 chain by BMP-1 and proprotein convertase(s) releases endotrophin in fragments of different sizes

Stefanie Elisabeth Heumüller, Maya Talantikite, Manon Napoli, Jean Armengaud, Matthias Mörgelin, Ursula Hartmann, Gerhard Sengle, Mats Paulsson, Catherine Moali and Raimund Wagener

J. Biol. Chem. 2019, 294:13769-13780.
doi: 10.1074/jbc.RA119.008641 originally published online July 25, 2019

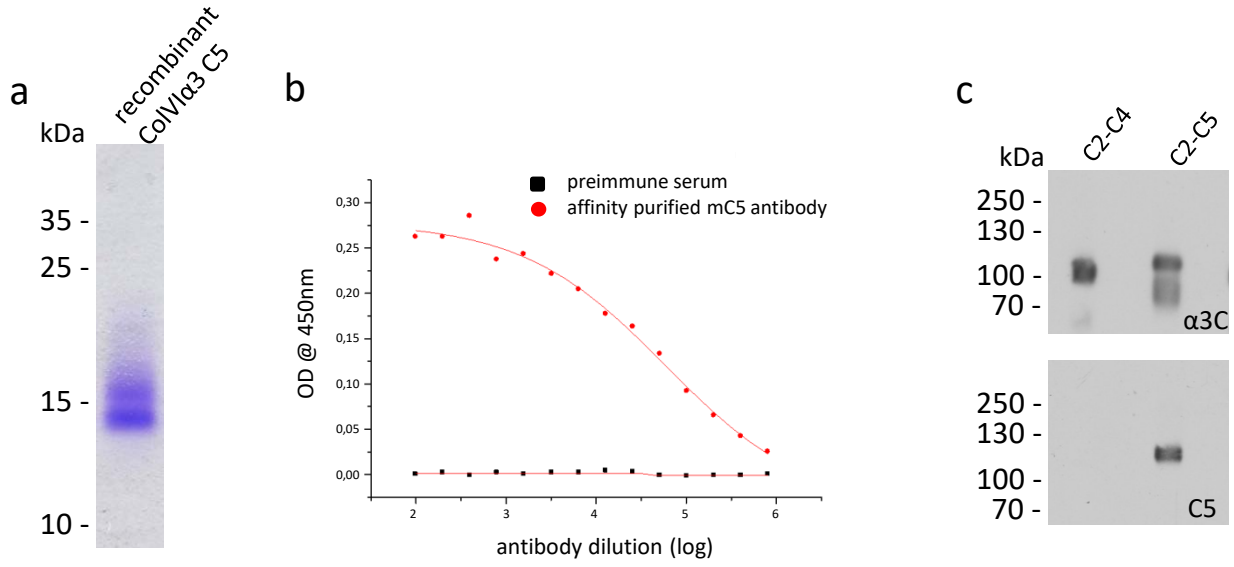

Supplemental Figure 1. Characterization of the specificity of the murine C5 antibody. a, Coomassie stained SDS-PAGE of the recombinant murine collagen VI α3 C5 protein carrying an N-terminal extension harbouring the BMP-1 cleavage site. b, Antibody titer determination of the affinity purified antiserum by ELISA. Plates were coated with 1 µg per well and antibodies were diluted as indicated. OD, optical density. Black filled squares, rabbit pre-immune sera; red filled circles, rabbit α3 C5 antibodies. c, immunoblots of recombinant collagen VIα3 C2-C4 and C2-C5 fragments probed with the murine C5 affinity purified antibody (lower panel) and an antibody (α3C) that detects the C1-C5 fragment (Maass et al., J Biol Chem. **291**, 5247–5258 (2016)), upper panel. The specificity is further demonstrated by immunoblots on serum and plasma shown in Fig. 2 a and b (main text). The antibody characterization is also representative for that performed for the antibody against the human C5.

Supplemental Figure 2. Immunofluorescence microscopy of day 1 to 6 primary dermal fibroblast cultures with antibodies against the N-terminus (red) and the C5 domain (green) of the collagen VI α3 chain. Bar = 50 µm.